

## Anisotropic Latent Heat of Vortex-Lattice Melting in Untwinned $\text{YBa}_2\text{Cu}_3\text{O}_{7-\delta}$

A. Schilling,<sup>1</sup> R. A. Fisher,<sup>1</sup> N. E. Phillips,<sup>1</sup> U. Welp,<sup>2</sup> W. K. Kwok,<sup>2</sup> and G. W. Crabtree<sup>2</sup>

<sup>1</sup>Lawrence Berkeley National Laboratory and Department of Chemistry, University of California, Berkeley, California 94720

<sup>2</sup>Science and Technology Center for Superconductivity, Argonne National Laboratory, Argonne, Illinois 60439

(Received 27 February 1997)

We report a distinct thermal signature of the first-order vortex-lattice melting for the external magnetic field  $H$  both parallel and perpendicular to the  $c$  axis of an untwinned  $\text{YBa}_2\text{Cu}_3\text{O}_{7-\delta}$  single crystal. Latent heats and discontinuities in specific heat were observed for each configuration. The entropies of melting and the melting lines  $H_m(T)$  both scale with an anisotropy parameter  $\gamma \approx 8$ . The specific heat of the vortex fluid is considerably larger than that of the vortex solid (by up to 2 mJ/mole K<sup>2</sup>), which is not explained by simple arguments based on counting the numbers of thermodynamic degrees of freedom. [S0031-9007(97)03400-5]

PACS numbers: 74.25.Bt, 74.60.Ge, 75.30.Gw

There is currently considerable effort, both theoretical and experimental, directed to elucidation of the “solid-liquid” transition that occurs at a phase boundary  $H_m(T)$  within the vortex state of cuprate superconductors. Thermodynamic information has been obtained mainly by magnetization measurements, on single crystals of  $\text{Bi}_2\text{Sr}_2\text{CaCu}_2\text{O}_8$  [1,2] and  $\text{YBa}_2\text{Cu}_3\text{O}_{7-\delta}$  [3,4]. The observation of associated thermal effects requires high-precision measurements on very high-quality crystals [5]. The first measurements that showed *any* thermal effect at  $H_m(T)$ , on twinned single crystals of  $\text{YBa}_2\text{Cu}_3\text{O}_{7-\delta}$ , indicated slight but clearly resolved increases  $\Delta C$  in the specific heat  $C$  for external magnetic fields  $H$  parallel to the  $c$  axis [6]. A similar, but somewhat larger, effect in another twinned crystal was reported later [7]. The earliest thermal measurements to reveal a *first-order* phase transition from the vortex lattice to the vortex-fluid phase gave a latent heat  $L \approx 0.5k_B T$  per vortex per superconducting layer in untwinned  $\text{YBa}_2\text{Cu}_3\text{O}_{7-\delta}$  for  $H \parallel c$ , and thermodynamic consistency was proven by a comparison with magnetization data for the same crystal [8]. A similar estimate for  $L$  was later reported by other authors [9,10], but the latent heat was observed only for  $\mu_0 H \geq 6$  T and was not thermodynamically consistent with the magnetization data.

Transport-property measurements have suggested the occurrence of a first-order transition also for a near- $H \perp c$  geometry in  $\text{YBa}_2\text{Cu}_3\text{O}_{7-\delta}$  [11,12], and the angular-dependent scaling of the melting line in the magnetic phase diagram of  $\text{YBa}_2\text{Cu}_3\text{O}_{7-\delta}$  has been investigated [12–14]. However, it has not been established whether or not there is a latent heat of vortex-lattice melting in the moderately anisotropic  $\text{YBa}_2\text{Cu}_3\text{O}_{7-\delta}$  in any geometry other than  $H \parallel c$ . Recent magnetization data for the highly anisotropic  $\text{Bi}_2\text{Sr}_2\text{CaCu}_2\text{O}_8$  [15] show a discontinuity in magnetization that persists, with increasing angle  $\Theta$  between  $H$  and  $c$ , from  $H \parallel c$  almost to  $H \perp c$ . The dependencies of the latent heats  $L$  on the orientation of  $H$  are expected to be quite different in the two systems, however, as are the phase diagrams

themselves. In the context of the earlier work, and because the “superconducting layers” perpendicular to the vortex lines, which might determine vortex segmentation and thus the number of degrees of freedom for thermodynamic quantities for  $H \parallel c$ , are not present for  $H \perp c$ , specific-heat measurements for  $H \perp c$  are of considerable interest. We report here more detailed specific-heat investigations at the vortex-lattice melting line of untwinned  $\text{YBa}_2\text{Cu}_3\text{O}_{7-\delta}$  that give  $L$  and  $\Delta C$  for both  $H \parallel c$  and  $H \perp c$ .

The untwinned  $\text{YBa}_2\text{Cu}_3\text{O}_{7-\delta}$  crystal (3.3 mg,  $T_c \approx 92$  K) was used earlier to measure the latent heat of vortex-lattice melting for  $H \parallel c$  [8]. The specific-heat  $C(H, T)$  data were obtained by the method described in Refs. [5] and [16].  $C(H, T)$  was measured for  $\Theta = 0^\circ \pm 4^\circ$  ( $H \parallel c$ ) and  $90^\circ \pm 2^\circ$  ( $H \parallel a$ ). The magnetization  $M(H, T)$  was detected with a commercial SQUID magnetometer (Quantum Design).

The specific-heat data for  $H \parallel c$  are displayed in Fig. 1 as  $C/T$  vs  $T$ . To visualize details in  $C/T$  more clearly, we have subtracted the data taken in zero magnetic field, and plotted the difference in Figs. 2(a) and 2(b) for  $H \parallel c$  and  $H \parallel a$ , respectively. The inset of Fig. 1 shows data for  $\mu_0 H = 1$  T  $\parallel c$  and  $\mu_0 H = 8$  T  $\parallel a$ . The two curves are almost identical, not only in their overall temperature dependence along the gradual crossover from the normal to the superconducting state, but also in the position, the amplitude, and the shape of a first-order-like feature that we ascribe to vortex-lattice melting. In Fig. 3 the comparison of specific-heat data for the two geometries is extended to other magnetic fields. In larger fields (i.e.,  $\mu_0 H > 4$  T  $\parallel a$  and  $\mu_0 H > 0.5$  T  $\parallel c$ ), both the shape of the peaks and the temperatures at which the specific-heat features occur coincide reasonably well if we compare pairs of curves that belong to external magnetic-field strengths differing by a factor 8 for the respective geometries. Below  $\mu_0 H = 4$  T  $\parallel a$  and  $\mu_0 H = 0.5$  T  $\parallel c$  the first-order-like features vanish in the instrumental noise. Nevertheless, step-like increases  $\Delta C/T$  can still be resolved for both

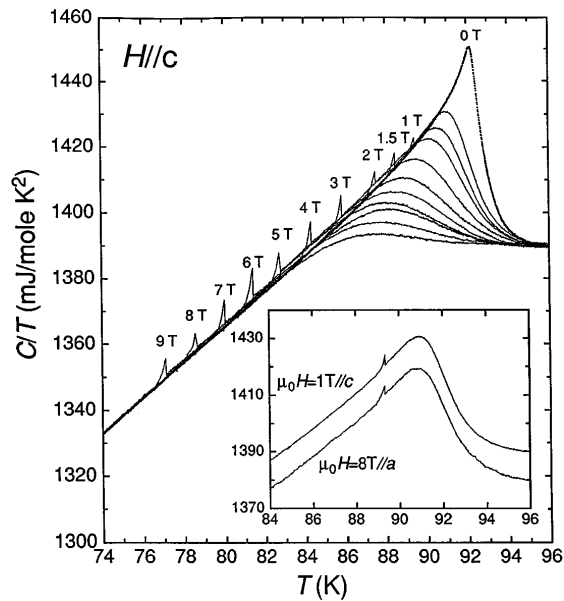


FIG. 1. Total specific heat of an untwinned  $\text{YBa}_2\text{Cu}_3\text{O}_{7-\delta}$  single crystal for  $H \parallel c$ . The numbers on top of the peaklike specific-heat features indicate the strength of the externally applied magnetic field. The inset shows representative data for  $\mu_0 H = 1 \text{ T} \parallel c$  and  $\mu_0 H = 8 \text{ T} \parallel a$  (shifted vertically by  $-10 \text{ mJ/mole K}^2$  for clarity).

configurations. As a consequence of the apparent scaling of these features, the melting fields  $H_m(T)$  in the  $H$ - $T$  phase diagram differ by a factor  $\approx 8$  for the two configurations. An empirical power-law fit to all the data with  $H_m = H_0(1 - T/T_c)^n$  for  $H \parallel c$  and  $H_m = \gamma H_0(1 - T/T_c)^n$  for  $H \parallel a$  gives  $\mu_0 H_0 = (87.3 \pm 3.1) \text{ T}$ ,  $T_c =$

$(91.87 \pm 0.04) \text{ K}$ ,  $n = (1.24 \pm 0.02)$ , and an anisotropy ratio  $\gamma = (m_c/m_{ab})^{1/2} = (7.76 \pm 0.15)$ , with the effective charge-carrier masses  $m_c$  and  $m_{ab}$  for current transport  $\parallel c$  and  $\perp c$ , respectively [14,17,18]. This latter value is consistent with the results of other experiments probing the angular dependence of vortex-lattice melting in  $\text{YBa}_2\text{Cu}_3\text{O}_{7-\delta}$  ( $\gamma \approx 7.4\text{--}8.7$  [12,14,19]).

The latent heats  $L = T\Delta S$  can be obtained by integrating the area under the peaks in the  $C/T$  vs  $T$  curves [16]. At a fixed  $T$ , the entropy discontinuity  $\Delta S$  per unit volume is approximately the same for both geometries [see Fig. 4(a), inset], indicating that  $\Delta S/H_m$  (which is proportional to  $\Delta S$  per vortex) scales with a factor of the order of  $\gamma$ . It has become a standard procedure to use the unit “per vortex per superconducting layer” (with the spacing of the layers usually taken as the distance  $c$  between the  $\text{CuO}_2$  double layers) for latent heats measured for  $H \parallel c$ , although in the quasi-3D system  $\text{YBa}_2\text{Cu}_3\text{O}_{7-\delta}$  one independent vortex segment contributing additional degrees of freedom may extend over several

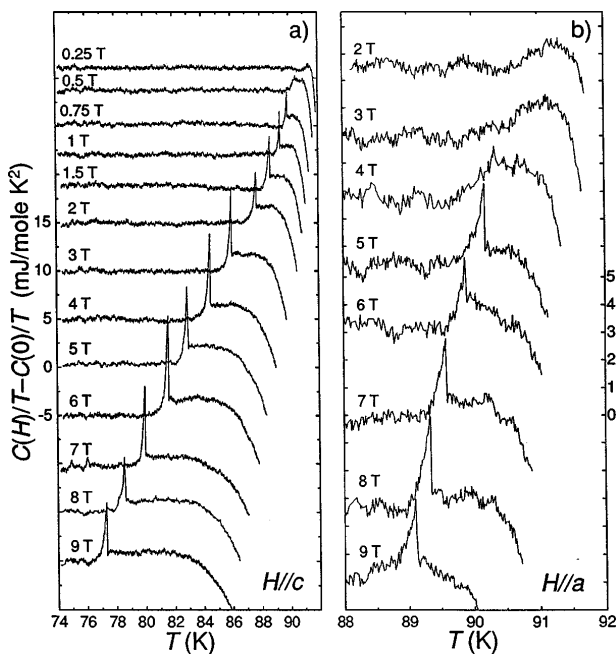


FIG. 2. Specific-heat differences  $C(H)/T - C(0)/T$  vs  $T$ , for  $H \parallel c$  (a) and  $H \parallel a$  (b). In each figure, the curves have been shifted arbitrarily for clarity.

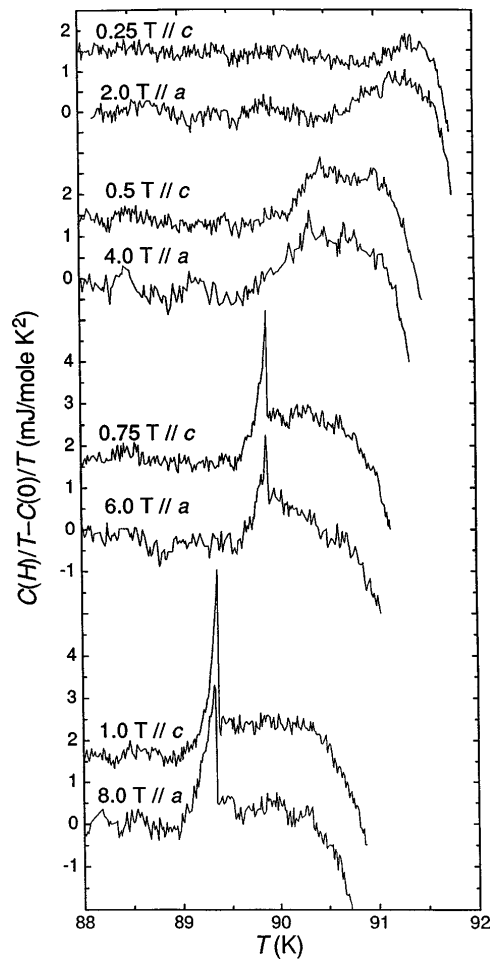


FIG. 3. Comparison between the specific-heat differences  $C(H)/T - C(0)/T$  measured in various external magnetic fields, for  $H \parallel c$  (upper curves, shifted by  $+1.5 \text{ mJ/mole K}^2$ ) and  $H \parallel a$  (lower curves). The magnetic-field values for each pair of curves differ by a factor 8.

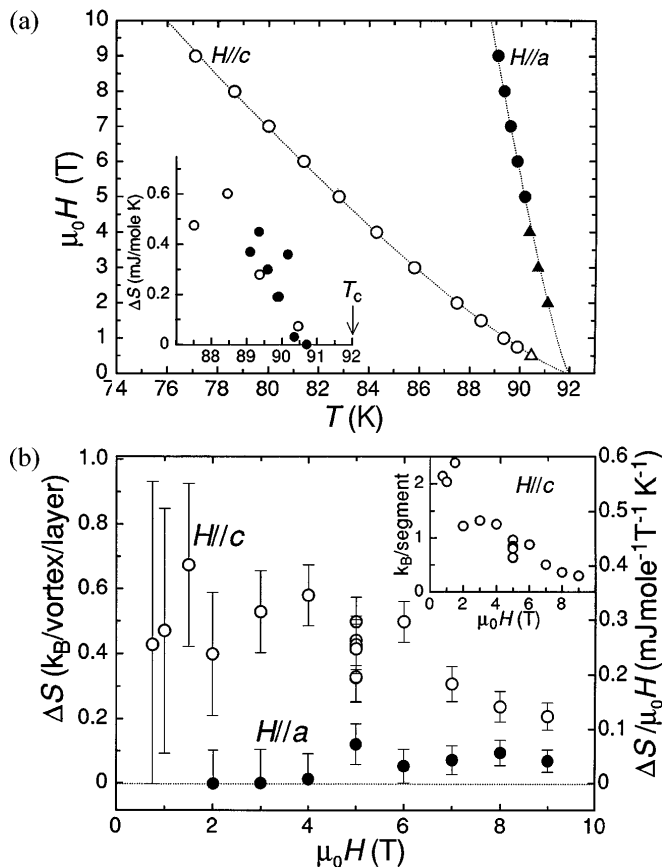


FIG. 4. (a) Vortex-lattice transition lines  $H_m(T)$  for  $\text{YBa}_2\text{Cu}_3\text{O}_{7-\delta}$  for  $H \parallel c$  (open symbols) and  $H \parallel a$  (filled symbols). Circles correspond to first-order melting, while triangles reflect the positions of step-like features in  $C/T$  without a clearly detectable latent heat. The dotted lines correspond to an empirical power-law fit (see text). The inset displays  $\Delta S$  at vortex-lattice melting per mole  $\text{YBa}_2\text{Cu}_3\text{O}_{7-\delta}$  near  $T_c$  as a function of  $T$ . (b) Entropies of vortex-lattice melting, in units of  $(k_B/\text{vortex})/\text{superconducting layer}$  (left scale),  $\text{mJ mole}^{-1} \text{T}^{-1} \text{K}^{-1}$  (right scale), and  $k_B/\text{vortex segment}$  of the length  $a_0/\gamma$  (inset), for  $H \parallel c$  (open symbols) (see text). The filled symbols show the corresponding values for  $H \parallel a$  (right scale).

unit cells. This oversimplified way of counting degrees of freedom would also imply that  $L$  vanishes for  $H \perp c$  because “superconducting layers” perpendicular to the vortex lines are not present in this geometry. A comparison of the elastic tilt energy accumulated along an individual vortex line with the interaction energy between neighboring vortices yields another estimate of the length of an independent vortex segment  $d(\Theta) = a_0 \gamma^{1/2} (\sin^2 \Theta + \gamma^2 \cos^2 \Theta)^{-3/4}$  [20], where  $a_0 \approx (\varphi_0/B)^{1/2}$  is the distance between the vortices,  $\varphi_0 = 2.07 \times 10^{-15} \text{ V s}$  is the magnetic-flux quantum, and  $B$  is the magnetic induction. As a consequence,  $\Delta S$  for  $H \parallel c$  ( $\Theta = 0^\circ$ ) should be larger than  $\Delta S$  for  $H \perp c$  ( $\Theta = 90^\circ$ ) by a factor  $\gamma^{3/2}$ , if counted in the same units, which is in qualitative agreement with our experimental data [Fig. 4(b)]. However, the marked  $H$  dependence of  $\Delta S$  for  $H \parallel c$  and the considerable experimental uncertainty in  $\Delta S$  for  $H \parallel a$

[see Fig. 4(b)] make a direct quantitative comparison between the two sets of data somewhat difficult. In Fig. 4(b), we compare  $\Delta S$  for  $H \parallel c$  in different units:  $(k_B/\text{vortex})/\text{superconducting layer}$  with interlayer separation  $s = c = 11.7 \text{ \AA}$ ,  $\text{mJ mole}^{-1} \text{T}^{-1} \text{K}^{-1}$ , and  $k_B/\text{vortex segment}$  of the length  $a_0/\gamma$  for  $H \parallel c$  (inset). Although the latter way of counting does not change the order of magnitude of  $\Delta S$ , it has a significant influence on its  $T$  dependence, introducing a strong increase near  $T_c$  (i.e.,  $H \rightarrow 0$ ), which is very similar to the trend that has been observed for  $\Delta S$  in  $\text{Bi}_2\text{Sr}_2\text{CaCu}_2\text{O}_8$  [2].

It is worthwhile mentioning that for a *perfect*  $H \perp c$  geometry (i.e., with an accuracy in  $\Theta$  that is significantly better than  $1^\circ$ ), no first-order transition should be observed [21]. The intrinsic-pinning effect, i.e., the localization of the vortices between the  $\text{CuO}_2$  double layers, has been demonstrated to broaden the sharp resistivity features associated with vortex-lattice melting for  $\Theta > 89.5^\circ$  [22].

In addition to the distinct peaks in  $C/T$  due to the latent heat that are visible in Figs. 1 and 2, a nearly step-like increase in the specific heat occurs at the vortex-lattice melting, by typically  $\Delta C/T \approx 1.5 \text{ mJ/mole K}^2$  for  $H \parallel c$ . Similar increases in  $C/T$  upon transforming the vortex solid to a fluid have been reported previously [6,7,10], with or without an accompanying first-order peak in the specific-heat data. A discontinuity in  $C/T$  is not unexpected; it is observed at the melting transition of most conventional solids. In Fig. 5 we have plotted the differences in  $C/T$  between the vortex fluid and the vortex-solid phases, both for  $H \parallel c$  and  $H \perp c$ .

Below the melting line, the vortex-lattice is very susceptible to pinning, and hence thermodynamic equilibrium is not *a priori* guaranteed. To check thermodynamic consistency of the  $H \parallel c$  data we compare them with  $(\partial M/\partial T)_H$  data measured on the same sample that

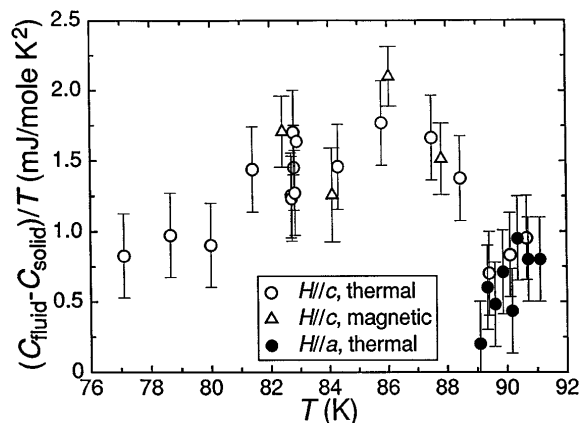


FIG. 5. Specific-heat difference  $\Delta C/T$  between the vortex fluid and the vortex-solid phases of  $\text{YBa}_2\text{Cu}_3\text{O}_{7-\delta}$  for  $H \parallel c$  (open symbols) and  $H \parallel a$  (filled symbols). The triangles correspond to estimates of  $\Delta C/T$  for  $H \parallel c$  based on magnetization  $M(T)$  measurements on the same sample and using Eq. (1) in the text. Experimental uncertainties in some of the terms in Eq. (1) are included in the error bars.

are within the experimental accuracy reversible [23]. Taking the total derivative of the Clapeyron equation  $\Delta S = -\Delta M dH_m/dT$  along  $H_m(T)$  with respect to  $T$ , we find for a first-order transition the relation

$$\Delta \left( \frac{C}{T} \right) + \Delta \left( \frac{\partial M}{\partial T} \right)_H \frac{dH_m}{dT} + \frac{d\Delta M}{dT} \frac{dH_m}{dT} + \Delta M \frac{d^2 H_m}{dT^2} = 0, \quad (1)$$

where  $\Delta M(T)$  is the  $T$ -dependent discontinuity in  $M$  at the melting line  $H_m(T)$  as reported in Refs. [4] and [8]. The estimate obtained for  $\Delta C/T$  is also shown in Fig. 5. The good agreement of the data suggests that the  $\Delta C/T$  steps reported here for  $H \parallel c$  represent thermodynamic-equilibrium properties of the vortex matter of  $\text{YBa}_2\text{Cu}_3\text{O}_{7-\delta}$ . The data for the  $H \perp c$  geometry (see Fig. 5), however, are not accurate enough to check thermodynamic consistency, or to reliably examine angular-dependent scaling of  $\Delta C/T$ .

To explain why the specific heat of the vortex matter increases upon melting one is tempted to invoke an increase in the number of vortices due to the discontinuity in the magnetic-flux density  $\Delta B = 4\pi\Delta M$ , and/or a change of the dynamics of the vortex lattice. These scenarios produce, under reasonable assumptions,  $\Delta C/T$  shifts that are by far too small to explain the experimental observations: The fraction of added vortices due to an increase  $\Delta B \approx 0.3$  G [3,4,8] is only  $\approx 10^{-5}$  in  $\mu_0 H = 5$  T. Taking  $\Delta C/T$  at  $T_c$  ( $\approx 52$  mJ/mole  $\text{K}^2$ ; see Fig. 1), as an upper limit for the total electronic specific heat, the added vortices would contribute to  $C/T$  with an increase  $\Delta C/T = 5 \times 10^{-4}$  mJ/mole  $\text{K}^2$  at most. A hypothetical increase in the number of degrees of freedom per vortex per layer (say, by  $n$ ) when the vortex solid melts would cause a shift in  $C$  that is of the order of  $nk_B$  per vortex per layer, where  $n$  cannot be significantly larger than unity (here,  $k_B = 1.38 \times 10^{-23}$  J/K is the Boltzmann constant). In  $\mu_0 H = 5$  T we estimate  $\Delta C/T = 1.7 \times 10^{-2}$  mJ/mole  $\text{K}^2$  if  $n = \frac{1}{2}$ . To explain the experimentally observed shifts one would have to invoke 80–100 additional degrees of freedom per vortex per superconducting layer, which is unrealistic, and the situation becomes even more unlikely for lower magnetic fields because the vortex density decreases with decreasing  $H$ , but  $\Delta C/T$  remains large down to  $\mu_0 H = 1.5$  T (i.e., up to  $T = 88.4$  K; see Fig. 5). One may argue more generally that the effective Debye temperature  $\Theta_D$  of the vortex matter changes on melting, thereby causing a change in the vortex specific heat. The maximum change in  $C$  that can occur in this scenario is the total vortex specific heat itself, that is largest in the high-temperature Dulong-Petit limit  $T \gg \Theta_D \approx 7$ –20 K [24,25]. This quantity amounts to only 1 or 2  $k_B$  per vortex per layer, respectively, depending on the assumptions on the effective mass of the vortices [24–27], which is again by far too small to account for the observed changes in  $C/T$ .

One may argue instead that the geometrical vortex configuration changes significantly when the (nearly) triangular vortex lattice melts to a disordered fluid state. Therefore, geometrical factors (like the Abrikosov ratio  $\beta_A$  [28]) are expected to change their value upon melting, and may therefore alter the  $T$  dependence of the electronic free energy accordingly.

We would like to thank to Professor D. R. Nelson and Professor G. Blatter for stimulating discussions. A. S. would like to thank to the Schweizerische Nationalfonds zur Förderung der Wissenschaftlichen Forschung for Grant No. 8220-042855 and for previous support. The work at Berkeley and at Argonne, respectively, was supported by the Director, Office of Basic Energy Sciences, Materials Sciences Division of the U.S. Department of Energy under Contracts No. DE-AC03-76SF00098 and No. W-31-109-ENG-38 (U. W., W. K. K., G. W. C.).

- 
- [1] H. Pastoriza *et al.*, Phys. Rev. Lett. **72**, 2951 (1994).
  - [2] E. Zeldov *et al.*, Nature (London) **375**, 373 (1995).
  - [3] R. Liang *et al.*, Phys. Rev. Lett. **76**, 835 (1996).
  - [4] U. Welp *et al.*, Phys. Rev. Lett. **76**, 4809 (1996).
  - [5] A. Schilling and O. Jeandupeux, Phys. Rev. B **52**, 9714 (1995).
  - [6] A. Schilling *et al.*, *Proceedings of the 10th Anniversary HTS Workshop on Physics, Materials and Applications*, Houston, Texas, 1996, edited by B. Batlogg *et al.* (World Scientific, Singapore, 1996), pp. 349–352.
  - [7] M. Roulin *et al.*, Science **273**, 1210 (1996).
  - [8] A. Schilling *et al.*, Nature (London) **382**, 791 (1996).
  - [9] M. Roulin *et al.*, J. Low Temp. Phys. **105**, 1099 (1996).
  - [10] A. Junod *et al.*, Physica (Amsterdam) **275C**, 245 (1997).
  - [11] M. Charalambous *et al.*, Phys. Rev. B **45**, 5091 (1992).
  - [12] W. K. Kwok *et al.*, Phys. Rev. Lett. **69**, 3370 (1992).
  - [13] D. E. Farrell *et al.*, Phys. Rev. Lett. **64**, 1573 (1990).
  - [14] R. G. Beck *et al.*, Phys. Rev. Lett. **68**, 1594 (1992).
  - [15] B. Schmidt *et al.*, Phys. Rev. B **55**, 8705 (1997).
  - [16] A. Schilling *et al.*, in Proceedings of the M<sup>2</sup>S-HTSC-V Conference Beijing, China, 1997 (to be published).
  - [17] G. Blatter *et al.*, Phys. Rev. Lett. **68**, 875 (1992).
  - [18] L. J. Campbell *et al.*, Phys. Rev. B **38**, 2439 (1988).
  - [19] W. K. Kwok *et al.*, Physica (Amsterdam) **197B**, 578 (1994).
  - [20] G. Blatter *et al.*, Rev. Mod. Phys. **66**, 1125 (1994), see Eq. (2.176).
  - [21] L. Balents and D. R. Nelson, Phys. Rev. B **52**, 12951 (1995).
  - [22] W. K. Kwok *et al.*, Phys. Rev. Lett. **67**, 390 (1991).
  - [23] U. Welp *et al.* (unpublished).
  - [24] A. L. Fetter, Phys. Rev. B **50**, 13 695 (1994).
  - [25] G. Blatter and B. I. Ivlev, Phys. Rev. B **50**, 10 272 (1994).
  - [26] L. N. Bulaevskii and M. P. Maley, Phys. Rev. Lett. **71**, 3541 (1993).
  - [27] K. A. Moler *et al.*, J. Low Temp. Phys. **100**, 185 (1995).
  - [28] A. A. Abrikosov, Zh. Eksp. Teor. Fiz. **32**, 1442 (1957) [Sov. Phys. JETP **5**, 1174 (1957)].